

Irradiation Damage Determined Field Emission of Ion Irradiated Carbon Nanotubes

Jian-Hua Deng,*[†] Xing-Gang Hou,[†] Lin Cheng,[†] Fan-Jie Wang,[†] Bin Yu,[†] Guo-Zheng Li,[†] De-Jun Li,[†] Guo-An Cheng,*[‡] and Shaolong Wu[§]

[†]College of Physics and Materials Science, Tianjin Normal University, Tianjin 300387, People's Republic of China

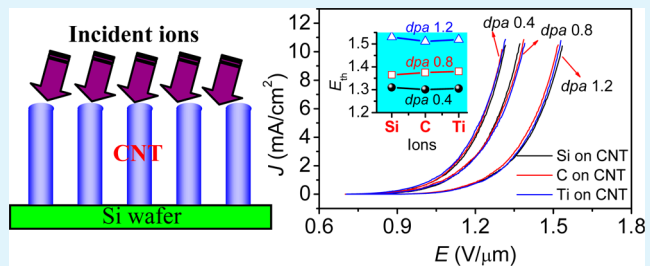
[‡]Key Laboratory of Beam Technology and Material Modification of Ministry of Education, Beijing Normal University, Beijing 100875, People's Republic of China

[§]Institute of Modern Optical Technologies, College of Physics, Optoelectronics and Energy, Soochow University, Suzhou 215006, People's Republic of China

Supporting Information

ABSTRACT: Figuring out the underlying relationship between the field emission (FE) properties and the ion irradiation induced structural change of carbon nanotubes (CNTs) is of great importance in developing high-performance field emitters. We report here the FE properties of Si and C ion irradiated CNTs with different irradiation doses. It is found that the FE performance of the ion irradiated CNTs ameliorates before and deteriorates after an irradiation-ion-species related dose. The improved FE properties are ascribed to the increased amount of defects, while the degraded FE performance is attributed to the great shape change of CNTs. These two structural changes are further characterized by a structural damage related parameter: dpa (displacement per atom), and the FE performance of the ion irradiated CNTs is surprisingly found to be mainly dependent on the dpa. The optimal dpa for FE of the ion irradiated CNTs is ~ 0.60 . We ascribe this to the low irradiation doses and the low substrate temperature that make the ion irradiation play a more important role in producing defects rather than element doping. Furthermore, the ion irradiated CNTs exhibit excellent FE stability, showing promising prospects in practical applications.

KEYWORDS: carbon nanotube, ion irradiation, dpa, field emission, defect



1. INTRODUCTION

Carbon nanotube (CNT), a quasi-one-dimensional material having outstanding mechanical and electrical properties,¹ has attracted much attention in a wide range of applications, such as thermal switches,² transistors,³ optical sensors,⁴ energy storage,^{5,6} and so on. CNTs can also serve as high-performance field emitters due to their high aspect ratio, excellent electrical conductivity, mechanical strength and chemical inertness. The field emission (FE) properties of CNTs have been intensively studied in recent years.^{7,8} Compared to some other good emitters such as single-layer graphenes,⁹ nanofibers,¹⁰ and nanotips,¹¹ CNTs have lower turn-on electric field (E_{on} , applied field at 10 μ A/cm²) and threshold field (E_{th} , applied field at 10 mA/cm²). These advantages make CNTs good candidates in practical applications such as flat panel displays,¹² X-ray tubes,¹³ and lamps.¹⁴ Enormous effort has so far been taken to modify the FE response of CNTs. Common strategies are decreasing the work function by element doping,¹⁵ introducing new active emission sites by compositing,^{16,17} chemical processing,¹⁸ and so on. Ion irradiation is another widely used approach. It has advantages in modifying the FE properties of CNTs by precisely controlling the irradiation doses. The irradiated CNTs

usually have lower E_{on} and E_{th} ¹⁹ and good stability.²⁰ However, the underlying relationship between the structure and the FE properties of ion irradiated CNTs needs to be further understood. The roles that element doping and structural damage play in improving the FE performance of ion irradiated CNTs need to be clearly identified.

In the present study, FE properties of Si and C ion irradiated CNTs are investigated. They can be precisely modified by changing the irradiation doses. The FE improvement and degradation induced by the ion irradiation are explained on the basis of structural analyses. Furthermore, the relationship between the FE performance and the structural damage of the ion irradiated CNTs is discussed.

2. EXPERIMENTAL SECTION

The CNTs were prepared on Si wafers by using thermal chemical vapor deposition.¹⁶ The prepared CNTs were then irradiated by energetic ions using a metal vapor vacuum arc ion source system, at a

Received: January 18, 2014

Accepted: March 12, 2014

Published: March 12, 2014



base pressure of $\sim 5 \times 10^{-4}$ Pa.²¹ Figure 1 schematically shows the ion irradiation on the CNTs. The samples were attached on a specimen

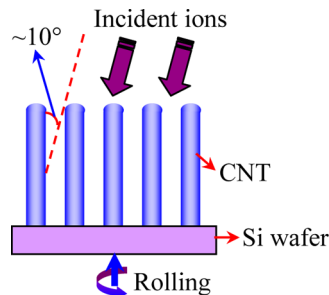


Figure 1. Schematic of the ion irradiation on CNTs with an incident angle of $\sim 10^\circ$.

holder, which was rolling during the irradiation to improve the uniformity of the irradiated areas. Si and C were used as the incident ions. The incident energy and angle were 20 keV and $\sim 10^\circ$, respectively. After then, the irradiated CNTs were cooled to room temperature in vacuum. The experimental details for the CNT preparation and the ion irradiation can also be found in the Methods of the Supporting Information (pages S1–S3), and the corresponding images are shown in Supporting Information Figure S1 and S2.

Morphological changes to the CNTs because of the ion irradiation were studied using scanning electron microscopy (SEM) imaging. The fine structure of the CNTs before and after the ion irradiation was characterized using high resolution transmission electron microscopy (TEM). The defect analysis was performed by using Raman spectroscopy with a laser wavelength of 633 nm. Photoelectron spectrometer was used to measure the work function of our samples.

The FE tests were carried out by using a parallel diode-type setup in a vacuum chamber ($\sim 10^{-7}$ Pa). The details for the sample characterizations and the FE tests are shown in Methods of the Supporting Information (pages S3–S5), and the corresponding images are shown in Supporting Information Figures S3 and S4.

3. RESULTS AND DISCUSSION

3.1. FE Properties of the Si and C Ion Irradiated CNTs.

It should be mentioned first that the as-grown CNTs used for the ion irradiation have similar morphology. They were prepared under the same conditions and usually at the same time. We have observed several as-grown CNTs, they show no much difference, as seen from SEM images shown in Figure S5 of the Supporting Information (page S5), which shows the side-view SEM image of 8 as-grown CNT arrays. All of the CNTs are well-aligned and $\sim 20 \mu\text{m}$ in length. The FE properties of the as-grown, Si and C ion irradiated CNTs were measured. We choose Si in thinking that the SiC compound, which has a low work function of 3.5 eV,²² can decline the work function of CNTs and thus improve their FE performance. Different from the Si, the C ion irradiation involves no element doping, it thus can help us understand the influence of Si doping on the FE properties of CNTs. Prior to FE tests, all the samples were aged at constant applied fields (E) for 5 h when the emission current density (J) was around 10 mA/cm^2 . This aging process is believed to be helpful for removing any absorbates and burning out loosely attached CNTs on our emitters.^{23,24} In this research, four irradiation doses are chosen for the ion irradiation on CNTs. They are 5×10^{16} , 10×10^{16} , 15×10^{16} , and $25 \times 10^{16} \text{ cm}^{-2}$. For convenience, the corresponding Si and C ion irradiated CNTs are named as Si(C)–S, Si(C)–

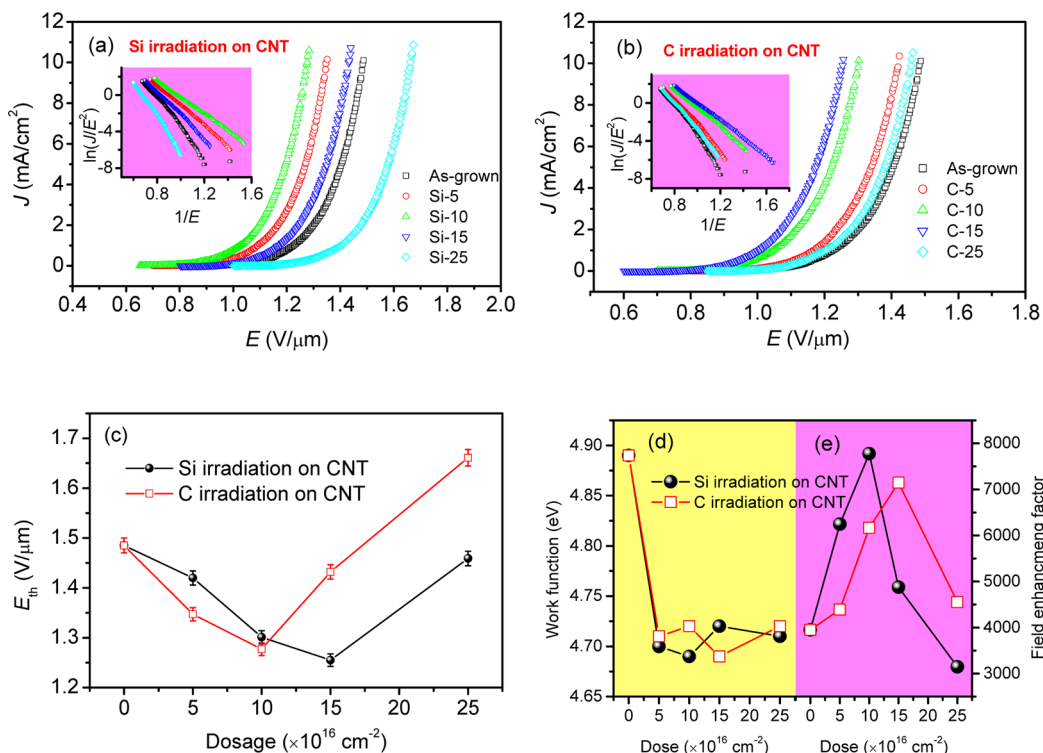


Figure 2. (a) FE J – E curves of Si ion irradiated CNTs with irradiation doses of 5×10^{16} (Si–5), 10×10^{16} (Si–10), 15×10^{16} (Si–15), and $25 \times 10^{16} \text{ cm}^{-2}$ (Si–25). Inset shows the classical F – N plots given in terms of $\ln(J/E^2)$ versus $1/E$. (b) FE J – E curves of C ion irradiated CNTs with irradiation doses of 5×10^{16} (C–5), 10×10^{16} (C–10), 15×10^{16} (C–15), and $25 \times 10^{16} \text{ cm}^{-2}$ (C–25), and the inset is the corresponding F – N plots. Comparison of the (c) E_{th} , (d) work function, and (e) field enhancement factor of the as-grown and ion irradiated CNTs with different irradiation doses.

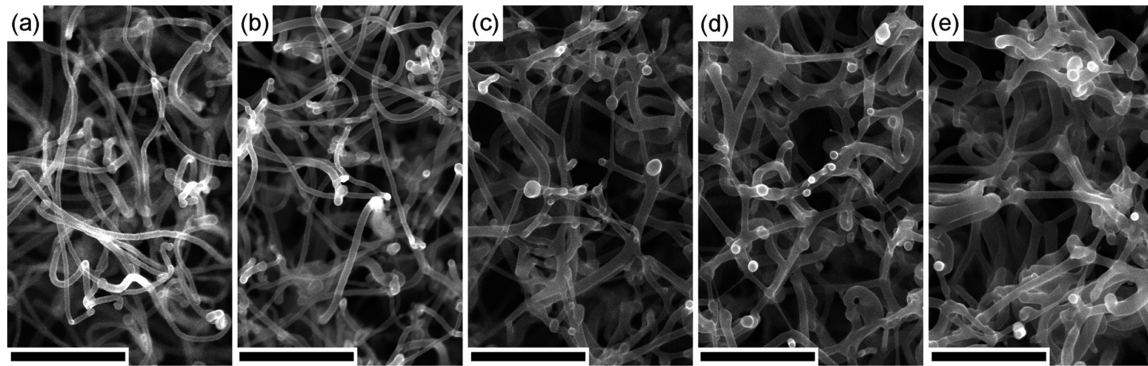


Figure 3. SEM images of the as-grown and Si ion irradiated CNTs showing the CNT shapes with irradiation doses of (a) 0, (b) 5×10^{16} , (c) 10×10^{16} , (d) 15×10^{16} , and (e) $25 \times 10^{16} \text{ cm}^{-2}$. All the scale bars are 500 nm.

10, Si(C)-15, and Si(C)-25, respectively. Figure 2a shows the FE response of the as-grown and the Si ion irradiated CNTs, expressed in terms of J versus E . For the as-grown sample, the E_{on} and E_{th} are 0.945 and 1.485 V/ μm , respectively. The ion irradiated CNTs by contrast, when the irradiation doses are less than $10 \times 10^{16} \text{ cm}^{-2}$, exhibit a gradually improved FE performance with the increase of irradiation doses, as seen from the left-shit of the $J-E$ curves. And then, the FE properties deteriorate with further increasing the irradiation doses. This change of FE performance with the irradiation doses can be clearly demonstrated by the change of E_{th} , as shown in Figure 2c. The error for the E_{th} is 1%. The details for obtaining this E_{th} error is shown in the Methods of the Supporting Information (pages S5 and S6), and the corresponding image is shown in Supporting Information Figure S6. The Si-10 sample has the best FE properties. It has a low E_{on} of 0.710 V/ μm and E_{th} of 1.277 V/ μm , far lower than those of the as-grown CNTs and Si ion irradiated CNTs with the other doses, not to mention a great many well-verified good emitters such as single-layer graphenes,⁹ nanofibers,¹⁰ and nanotips.¹¹

The FE $J-E$ curves of the C ion irradiated CNTs are shown in Figure 2b. With the increase of irradiation doses, they have a similar change as that for the Si ion irradiated CNTs: ameliorate before and deteriorate after a dose of $15 \times 10^{16} \text{ cm}^{-2}$, which can also be seen from the change of E_{th} shown in Figure 2c. The C-15 CNTs have the optimal FE properties. They have an extremely low E_{on} of 0.703 V/ μm and E_{th} of 1.255 V/ μm . These results indicate that the ion irradiation influences the FE behavior of the ion irradiated CNTs in a similar manner no matter what the ion species is. However, the optimal irradiation dose for FE is dependent on the ion species. The insets of Figure 2a and 2b show the Fowler-Nordheim ($F-N$) plots for the Si and C ion irradiated CNTs, respectively, given in terms of $\ln(J/E^2)$ versus $1/E$.²⁵ Each plot shows a linear relationship in the low- E regions, indicating that the emitted electrons are exactly extracted by the applied fields.²⁵ Figure 2d shows the work function of CNTs measured by using a photoelectron spectrometer. The ion irradiated CNTs have smaller work function with respect to the as-grown sample. This is ascribed to the ascended Fermi Level induced by the increased state density of defect after the ion irradiation.²⁶ However, the change of work function is negligible (from 4.69 to 4.72 eV) for the ion irradiated CNTs, which deviates from our anticipation that the Si ion irradiation will decline the work function of our samples. Furthermore, there is no much difference between the work function of the Si and C ion

irradiated CNTs. Since the C ion irradiation involves no element doping, thus the Si ion irradiation induced element doping is negligible here. We attribute this to the low irradiation doses and the low substrate temperature that hinders the formation of SiC compound. With the work function and the constant slopes of the $F-N$ plots in the low- E regions, the field enhancement factor (β) of the emitters can be calculated using the $F-N$ equation,²⁵ as shown in Figure 2e. It can be seen that the Si-10 and C-15 samples having the optimal FE properties have the largest β : 7776 and 7146, respectively. Both of them are far larger than that of the as-grown CNTs: 3949. Different from the small change of the work function, the change of β for the ion irradiated CNTs is outstanding, indicating that the FE properties of the ion irradiated CNTs are mainly determined by the structure related β rather than by the decline of work function. We consider that two structural changes, CNT shape and CNT microstructure, directly determine the FE performance of the ion irradiated CNTs.

3.2. CNT Shape Change with the Irradiation Doses. In this research, as-grown and ion irradiated CNTs with different irradiation doses were observed by SEM for comparison. In the following, discussions on the shape change of CNTs with the irradiation doses are given on the basis of the SEM images of Si ion irradiated CNTs, mainly due to the shape change of C ion irradiated CNTs is not so obvious when the irradiation doses are relatively low, as seen from the SEM images of C ion irradiated CNTs shown in Figure S7 of the Supporting Information (page S6), and the reason behind this will be explained later. Figure 3a shows the top-view SEM image of the as-grown CNTs. They are well-separated at the tips and have diameters of 40–60 nm. Figure 3b–e is the top-view SEM images of the Si ion irradiated CNTs, showing their shape change with the increase of irradiation doses. In comparison with the as-grown CNTs, the CNT shape change of the Si-5 sample is negligible. The irradiated CNTs are still well-separated (Figure 3b). This morphology is believed to be beneficial for FE because of the large amount of active emission sites. Figure 3c shows the CNT shape of the Si-10 sample. It changes a lot as compared to the as-grown and the Si-5 samples. First, a few CNTs begin to melt together due to the excessive energy deposition.²⁷ Furthermore, the diameter of the ion irradiated CNTs increases. With further increasing the irradiation doses, more and more CNTs are melted together and the thickening of CNTs becomes outstanding, as shown in Figure 3d and e. These two morphological changes are detrimental to the FE of CNTs. The melting of CNT tips

greatly decreases the amount of active emission sites, and the thickening of CNTs will decrease the β , both of them will lead to the degradation of the FE properties of CNTs. To sum up, the CNT shape change is not obvious when the irradiation doses are lower than the critical value (10×10^{16} and $15 \times 10^{16} \text{ cm}^{-2}$ for the Si and C ion irradiation, respectively), thus its influence on the FE performance of CNTs is limited. However, the shape change greatly deteriorates the FE properties of CNTs when the irradiations doses are further increased due to the decreased amount of active emission sites.

3.3. Microstructure Change of the Ion Irradiated CNTs.

Since the shape change is detrimental to the FE performance of CNTs, there must be some other structural changes that are responsible for their improved FE properties. We attribute the FE improvement to the microstructure changes of CNTs. We used high-resolution TEM imaging to get insight into the possible microstructure changes of CNTs. The as-grown and the Si-10 CNTs were observed for comparison. Figure 4a and b shows the high-resolution TEM images of the as-grown and the Si-10 CNTs, respectively. It can be seen that they both have typical layered structure at the inner layers and a hollow core, but the ion irradiated CNT has more defects at the outer shells. It should be mentioned that most of the ion irradiated CNTs only have defected outer layers due to the small incident angle ($\sim 10^\circ$).

To further characterize the structure of CNTs, Raman spectroscopy was employed. Figure 4c shows the Raman spectra of the as-grown and the Si ion irradiated CNTs. All the five samples have two typical peaks: D peak (centered at $\sim 1322 \text{ cm}^{-1}$) and G peak (centered at $\sim 1584 \text{ cm}^{-1}$), which correspond with the defected and ordered graphite, respectively.^{28–30} The intensity ratio of the D peak and G peak (I_D/I_G) can be used to qualitatively evaluate the defect of CNTs.²⁸ It can be seen that the I_D/I_G ratio increases with the increase of Si ion irradiation doses, indicating that more defects are produced by the incident ions when the irradiation doses are increased. It is interesting that the increase of the I_D/I_G ratio is slight when the irradiation doses are sufficiently high. We attribute this to the fact that the excessive energy deposition induced annealing of defects makes part of the defects annealed in these high-dose conditions,²⁷ thus even there are newly produced defects, the total amount of defects increases slightly.

The FE improvement induced by the defects is schematically illustrated in Figure 4d. In comparison with the planar sp^2 -hybridized carbon of CNTs, the distorted sp^3 -hybridized carbon of defects is believed to be helpful for FE. The electron transferring traces are increased due to the introduction of defects, especially vacancy-related defects.³¹ For a flawless as-grown CNT, the electron transferring mainly occurs at the CNT tip, while for a defected one, even the tube wall can serve as extra active emission sites. Therefore, we consider that the presence of defects is a key factor for the improved FE properties of the ion irradiated CNTs.

3.4. dpa Determined FE Performance of the Ion Irradiated CNTs.

The above results have shown that the FE properties of the ion irradiated CNTs are mainly influenced by the CNT shape and the amount of defects. In the following, these two structural changes are characterized by a structural damage related parameter, dpa (displacement per atom). This will help us construct a quantitative relationship between the FE performance and the structural damage of CNTs, and thus figure out the underlying causes for their FE improvement and degradation induced by the ion irradiation. The probability of

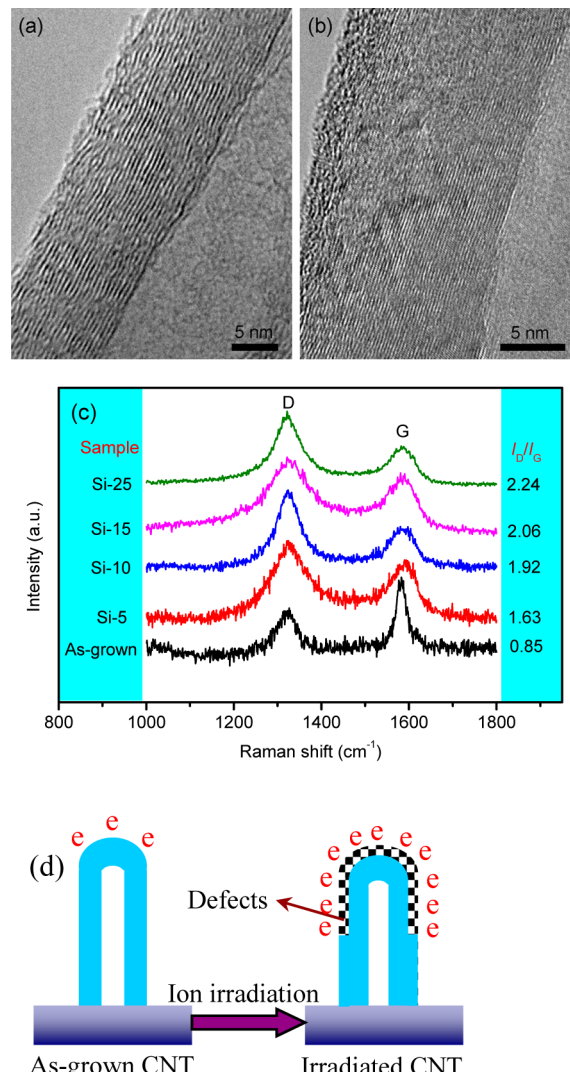


Figure 4. High-resolution TEM images of (a) as-grown and (b) Si-10 CNTs. (c) Raman spectra (laser wavelength = 633 nm) of the as-grown and the Si ion irradiated CNTs. The I_D and I_G are the intensity of D peak and G peak, respectively, and I_D/I_G is the intensity ratio of D peak and G peak. (d) Concept schematic of the enhanced FE from the defects of CNTs; “e” stands for the emitted electrons.

dpa is simulated using TRIM (transport of ions in matter) and calculated as follows:

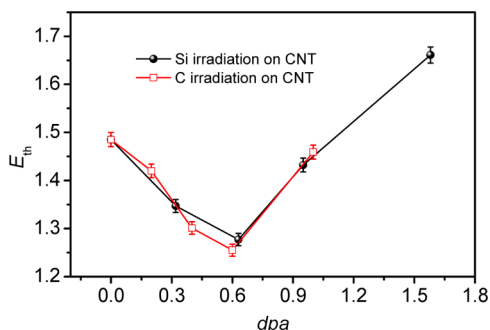
$$\text{dpa} = \frac{\Phi N_d}{N_{\text{atom}} l} \quad (1)$$

where $\Phi (\text{cm}^{-2})$ is the irradiation dose, N_d is the average displacement atoms per incident ion obtained by using the TRIM simulation, $N_{\text{atom}} (\text{cm}^{-3})$ is the atomic density of the CNTs calculated by $N_{\text{atom}} = 6.02 \times 10^{23} \rho_{\text{CNT}}/M_C$ (ρ_{CNT} is the density of CNTs, $\sim 1.4 \text{ g/cm}^3$,³² M_C is the atomic weight of carbon, 12 g/mol), and $l (\text{cm})$ is the incident depth of ions. Because of the shield of surrounding CNTs, the incident depth of the ions for our CNTs is $\sim 4 \mu\text{m}$ at the tips, which is obtained by using energy dispersive X-ray spectroscopy in our previous study.³³ Table 1 shows the dpa of the Si and C ion irradiated CNTs. It can be seen that the dpa increases monotonously with the irradiation doses, indicating an accompanied increase of the structural damage. The dpa values

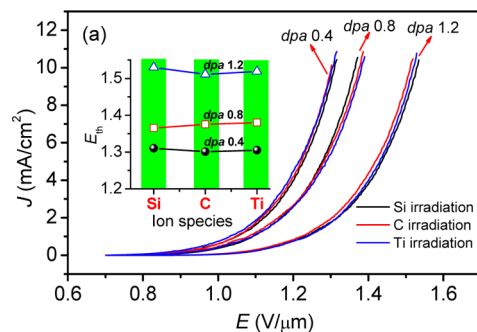
Table 1. Irradiation dpa of the Si and C ion irradiated CNTs with different irradiation doses

dose ($\times 10^{16} \text{ cm}^{-2}$)	5	10	15	25
dpa of Si on CNT	0.32	0.63	0.95	1.58
dpa of C on CNT	0.20	0.40	0.60	1.00

are different for different incident ions even if the irradiation doses are the same, mainly due to the fact that different ions have a different ability to create structural damage. This can be expressed by the different N_d values. The N_d values for the Si and C ion irradiation are 177 and 114, respectively. According to the definition of dpa (eq 1), this great difference in the N_d values directly results in the great difference in the dpa when the irradiation doses are the same. Together with the SEM and TEM observations presented before, the dpa here has 2-fold meanings: microstructure change and shape change of CNTs. The FE performance of the ion irradiated CNTs is replotted in terms of E_{th} versus dpa, as shown in Figure 5. We surprisingly

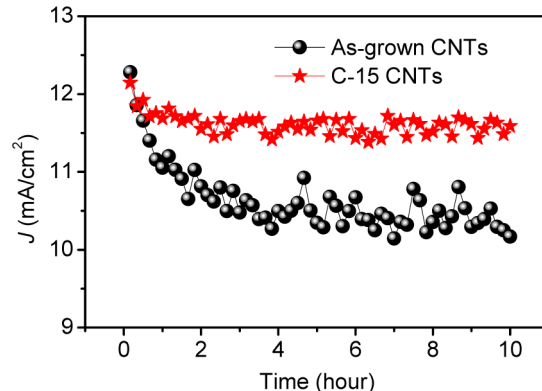
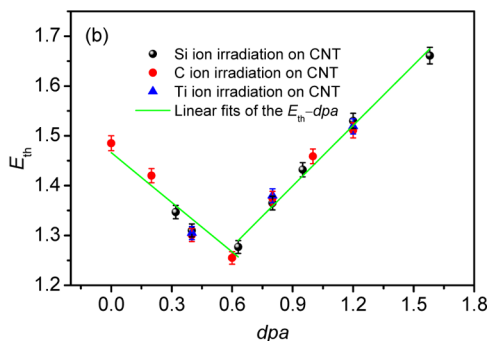
**Figure 5.** FE performance of the Si and C ion irradiated CNTs described in terms of E_{th} versus dpa.

find that the E_{th} has a major dependence on the dpa no matter what the ion species is. This is quite different from the previous findings that the E_{th} -dose relationship is dependent on the ion species (Figure 2c). The optical dpa for FE of the ion irradiated CNTs is ~ 0.60 . The FE performance of CNTs is improved when the dpa is smaller than 0.60 mainly because the increased amount of defects will introduce a great many active emission sites. Besides, the CNT shape change is negligible when the dpa is smaller than 0.60 (Figure 3a–c). However, when the dpa is larger than 0.60, the dramatic CNT shape change (Figure 3d and 3e) will greatly decrease the number of active emission sites, and thus degrade the FE performance of our emitters.

**Figure 6.** (a) FE $J-E$ curves of the Si, C, and Ti ion irradiated CNTs with irradiation dpa of 0.4, 0.8, and 1.2, the inset is the plots of the E_{th} of dpa 0.4, 0.8, and 1.2 samples as a function of the ion species, showing that the FE performance of the irradiated CNTs is independent of the ion species but dependent on the irradiation dpa. (b) The change of the E_{th} of Si, C, and Ti ion irradiated CNTs with the increase of irradiation dpa.

To further demonstrate the above dpa dependent FE behavior of CNTs, Ti ion irradiation on CNTs was performed for comparison. The incident angle and energy were the same as those used in the Si and C ion irradiation: $\sim 10^\circ$ and 20 kV, respectively. In this research, FE properties of Si, C, and Ti ion irradiated CNTs with dpa of 0.4, 0.8, and 1.2 were measured. Figure 6a shows the FE $J-E$ curves of these ion irradiated CNTs. It can be seen that the FE $J-E$ curves for the ion irradiated CNTs show no much difference when the dpa is the same no matter what the ion species is, indicating that the FE properties of the ion irradiated CNTs are mainly dependent on the dpa. This FE-dpa dependence can also be seen from the inset of Figure 6a: the ion irradiated CNTs with the same dpa have similar E_{th} . Figure 6b shows the E_{th} change of the Si, C, and Ti ion irradiated CNTs with the increase of irradiation dpa. It can be seen that the E_{th} changes almost monotonously before and after a critical dpa, which is ~ 0.60 in our study, and this change of E_{th} with the dpa is independent of the irradiation ion species. We ascribe this dpa dependent FE of the ion irradiated CNTs to the low irradiation doses of the incident ions and also the low substrate temperatures. They both make the ion irradiation plays a more important role in producing defects rather than element doping.

Longtime stable field electron transfer from emitters is of great importance in practical applications. In this research, FE stability of the as-grown CNTs and the ion irradiated CNTs having the best FE properties (the C-15 sample) were tested for comparison. Figure 7 shows the 10-h FE stability of these

**Figure 7.** 10-h FE stability of the as-grown and the C-15 CNTs, presented in terms of J versus time.

two samples when the J is around 10 mA/cm^2 . The stability plots are expressed in terms of J versus time. The FE currents were automatically recorded by a computer every 10 min. In order to observe the FE current change in the whole process, these samples were not subjected to an aging process before the FE stability tests, which is different from the obtaining of FE $J-E$ curves that all samples were preaged at constant applied fields for 5 h. We employ here a parameter J_{drop} to evaluate the FE stability of our samples. The J_{drop} is calculated by $(J_{\text{first}} - J_{\text{last}})/J_{\text{mean}}$ where the J_{first} , J_{last} , and J_{mean} are the first, the last, and the mean emission current densities during the 10-h tests. The FE stability testing results are shown in Table 2. It can be seen that

Table 2. FE Stability Testing Results of the As-Grown and C-15 CNTs

sample	E ($\text{V}/\mu\text{m}$)	J_{mean} (mA/cm^2)	J_{drop} (%)
as-grown	1.55	10.62	19.87
C-15	1.35	11.61	4.74

the J_{drop} for the C-15 CNTs is only 4.74%, far smaller than that of the as-grown CNTs (19.87%). In addition, the FE current degradation mainly occurs in the first few hours. The J_{drop} for the as-grown CNTs in the first 4 h is 16.76%, while for the C-15 CNTs in the first 1 h is 3.88%. And then, the FE current drop is small, especially for the C-15 CNTs, the FE current of which is almost constant. We attribute the current degradation in the first few hours to the Joule heating induced burning out of active emission sites,²⁴ which is helpful for the aging of our samples. The improved FE stability of the ion irradiated CNTs is attributed to the following two aspects. First, only CNTs that are severely defected are most likely to be burned out during FE, which directly leads to the current degradation. The ion irradiation can destroy part of those CNTs and thus improve the FE stability of CNTs. Second, the working applied fields for the as-grown and the C-15 CNTs are 1.55 and 1.35 $\text{V}/\mu\text{m}$, respectively. This decreased E can greatly decrease the probability that some loosely attached CNTs are pulled out from the substrates due to the electrostatic force,³⁴ which directly decreases the amount of active emission sites. Our results suggest that longtime stable FE from CNTs can be readily achieved by ion irradiation and aging for a few hours. The low operating E and the excellent FE stability have made our ion irradiated CNTs good candidates as high-performance field emitters.

4. CONCLUSIONS

We have demonstrated the FE properties of Si and C ion irradiated CNTs with different irradiation doses. They are found to be improved before and deteriorated after an irradiation-ion-species related dose. We attribute the FE improvement to the increased amount of defects that introduces new active emission sites. While the deteriorated FE performance is ascribed to the great shape change of CNTs, which directly decreases the active emission sites. The CNT shape change and microstructure change of the ion irradiated CNTs are further characterized by the dpa. The FE properties of CNTs are found to be mainly dpa-dependent. The optimal dpa for FE of the ion irradiated CNTs is ~ 0.60 . We ascribe this to the low irradiation doses and the low substrate temperature in our study that make the ion irradiation play a more important role in introducing defects rather than element doping. Furthermore, the ion irradiated CNTs have excellent

FE stability, far better than that of the as-grown CNTs, showing promising prospects in practical applications such as flat panel displays, X-ray tubes, and lamps.

■ ASSOCIATED CONTENT

S Supporting Information

The methods for CNT preparation, ion irradiation, structural characterization, and field emission, SEM images of as-grown CNTs and C ion irradiated CNTs, the method for the determination of the E_{th} error. This material is available free of charge via the Internet at <http://pubs.acs.org>.

■ AUTHOR INFORMATION

Corresponding Authors

*Phone: +86-22-23766519. E-mail: jhdeng1983@163.com.

*Phone: +86-10-62205403. E-mail: gacheng@bnu.edu.cn.

Notes

The authors declare no competing financial interest.

■ ACKNOWLEDGMENTS

This work was supported by the National Natural Science Foundation of China (Nos. 51302187, 51302188, 11204215, and 51272176), the National Basic Research Program of China (2010CB832905), the Tianjin High School Science & Technology Foundation (20120312), the Natural Science Foundation of Tianjin Normal University (5RL119), and partly by the Key Project of Tianjin Natural Science Foundation of China (Nos. 13JCZDJC33900 and 12JCYBJC32500).

■ REFERENCES

- Iijima, S. Helical Microtubules of Graphitic Carbon. *Nature* **1991**, *354*, 56–58.
- Sun, P. C.; Wu, Y. L.; Gao, J. W.; Cheng, G. A.; Chen, G.; Zheng, R. T. Room Temperature Electrical and Thermal Switching CNT/Hexadecane Composites. *Adv. Mater.* **2013**, *25*, 4938–4943.
- Ding, L.; Wang, Z. X.; Pei, T.; Zhang, Z. Y.; Wang, S.; Xu, H. L.; Peng, F.; Li, Y.; Peng, L. M. Self-Aligned U-Gate Carbon Nanotube Field-Effect Transistor with Extremely Small Parasitic Capacitance and Drain-Induced Barrier Lowering. *ACS Nano* **2011**, *5*, 2512–2519.
- Barone, P. W.; Baik, S.; Heller, D. A.; Strano, M. S. Near-Infrared Optical Sensors Based on Single-Walled Carbon Nanotubes. *Nat. Mater.* **2005**, *4*, 86–92.
- Jiang, Y. Q.; Wang, P. B.; Zang, X. N.; Yang, Y.; Kozinda, A.; Lin, L. W. Uniformly Embedded Metal Oxide Nanoparticles in Vertically Aligned Carbon Nanotube Forests as Pseudocapacitor Electrodes for Enhanced Energy Storage. *Nano Lett.* **2013**, *13*, 3524–3530.
- Chen, P.; Wu, X.; Lin, J.; Tan, K. L. High H_2 Uptake by Alkali-Doped Carbon Nanotubes Under Ambient Pressure and Moderate Temperatures. *Science* **1999**, *2*, 91–93.
- Fan, S. S.; Chapline, M. G.; Franklin, N. R.; Tombler, T. W.; Cassell, A. M.; Dai, H. J. Self-Oriented Regular Arrays of Carbon Nanotubes and Their Field Emission Properties. *Science* **1999**, *283*, 512–514.
- Zhu, L. B.; Sun, Y. Y.; Hess, D. W.; Wong, C. P. Well-Aligned Open-Ended Carbon Nanotube Architectures: An Approach for Device Assembly. *Nano Lett.* **2006**, *6*, 243–247.
- Wu, Z. S.; Pei, S. F.; Ren, W. C.; Tang, D. M.; Gao, L. B.; Liu, B. L.; Li, F.; Liu, C.; Cheng, H. M. Field Emission of Single-Layer Graphene Films Prepared by Electrophoretic Deposition. *Adv. Mater.* **2009**, *21*, 1756–1760.
- Weng, C. H.; Leou, K. C.; Wei, H. W.; Juang, Z. Y.; Wei, M. T.; Tung, C. H.; Tsai, C. H. Structural Transformation and Field Emission Enhancement of Carbon Nanofibers by Energetic Argon Plasma Post-treatment. *Appl. Phys. Lett.* **2004**, *85*, 4732–4734.

- (11) Tsai, C. L.; Chen, C. F.; Wu, L. K. Bias Effect on the Growth of Carbon Nanotips Using Microwave Plasma Chemical Vapor Deposition. *Appl. Phys. Lett.* **2002**, *81*, 721–723.
- (12) Wang, Q. H.; Yan, M.; Chang, R. P. H. Flat Panel Display Prototype Using Gated Carbon Nanotube Field Emitters. *Appl. Phys. Lett.* **2001**, *78*, 1294–1296.
- (13) Haga, A.; Senda, S.; Sakai, Y.; Mizuta, Y.; Kita, S.; Okuyama, F. A Miniature X-ray Tube. *Appl. Phys. Lett.* **2004**, *84*, 2208–2210.
- (14) Saito, Y.; Uemura, S. Field Emission from Carbon Nanotubes and its Application to Electron Sources. *Carbon* **2000**, *38*, 169–182.
- (15) Zhang, G.; Duan, W. H.; Wu, B. L. Effect of Substitutional Atoms in the Tip on Field-Emission Properties of Capped Carbon Nanotubes. *Appl. Phys. Lett.* **2002**, *80*, 2589–2591.
- (16) Deng, J. H.; Zheng, R. T.; Zhao, Y.; Cheng, G. A. Vapor-Solid Growth of Few-Layer Graphene Using Radio Frequency Sputtering Deposition and Its Application on Field Emission. *ACS Nano* **2012**, *6*, 3727–3733.
- (17) Deng, J. H.; Cheng, G. A.; Zheng, R. T.; Yu, B.; Li, G. Z.; Hou, X. G.; Zhao, M. L.; Li, D. J. Catalyst-Free, Self-Assembly, and Controllable Synthesis of Graphene Flake-Carbon Nanotube Composites for High-Performance Field Emission. *Carbon* **2014**, *67*, S25–S33.
- (18) Kung, S. C.; Hwang, K. C.; Lin, I. N. Oxygen and Ozone Oxidation-Enhanced Field Emission of Carbon Nanotubes. *Appl. Phys. Lett.* **2002**, *80*, 4819–4821.
- (19) Kyung, S. J.; Park, J. B.; Park, B. J.; Lee, J. H.; Yeom, G. Y. Improvement of Electron Field Emission from Carbon Nanotubes by Ar Neutral Beam Treatment. *Carbon* **2008**, *46*, 1316–1321.
- (20) Chen, G. H.; Shin, D. H.; Kim, S.; Roth, S.; Lee, C. J. Improved Field Emission Stability of Thin Multiwalled Carbon Nanotube Emitters. *Nanotechnology* **2010**, *21*, No. 015704.
- (21) Deng, J. H.; Yu, B.; Li, G. Z.; Hou, X. G.; Zhao, M. L.; Li, D. J.; Zheng, R. T.; Cheng, G. A. Self-Assembled Growth of Multi-Layer Graphene on Planar and Nano-Structured Substrates and its Field Emission Properties. *Nanoscale* **2013**, *5*, 12388–12393.
- (22) Da, D. A. *Vacuum Design Manual*, 3rd ed.; National Defense Industry Press: Lanzhou, China, 2004; P 1620.
- (23) Maiti, A.; Andzelm, J.; Tanpipat, N.; von Allmen, P. Effect of Adsorbates on Field Emission from Carbon Nanotubes. *Phys. Rev. Lett.* **2001**, *87*, No. 155502.
- (24) Dean, K. A.; Burgin, T. P.; Chalamala, B. R. Evaporation of Carbon Nanotubes During Electron Field Emission. *Appl. Phys. Lett.* **2001**, *79*, 1873–1875.
- (25) Fowler, R. H.; Nordheim, L. Electron Emission in Intense Electric Fields. *Proc. R. Soc. London, Ser. A* **1928**, *119*, 173–181.
- (26) Kim, G.; Jeong, B. W.; Ihm, J. Deep Levels in the Band Gap of the Carbon Nanotube with Vacancy-Related Defects. *Appl. Phys. Lett.* **2006**, *88*, No. 193107.
- (27) Terrones, M.; Terrones, H.; Banhart, F.; Charlier, J. C.; Ajayan, P. M. Coalescence of Single-Walled Carbon Nanotubes. *Science* **2000**, *288*, 1226–1229.
- (28) Tuinstra, F.; Koenig, J. L. Raman Spectrum of Graphite. *J. Chem. Phys.* **1970**, *53*, 1126–1130.
- (29) Ferrari, A. C.; Meyer, J. C.; Scardaci, V.; Casiraghi, C.; Lazzeri, M.; Mauri, F.; Piscanec, S.; Jiang, D.; Novoselov, K. S.; Roth, S.; Geim, A. K. Raman Spectrum of Graphene and Graphene Layers. *Phys. Rev. Lett.* **2006**, *97*, No. 197401.
- (30) Nemanich, R. J.; Solin, S. A. First- and Second-Order Raman Scattering from Finite-Size Crystals of Graphite. *Phys. Rev. B* **1979**, *20*, 392–401.
- (31) Gu, W. Emission Property of Carbon Nanotube with Defects. *Appl. Phys. Lett.* **2006**, *89*, No. 143111.
- (32) Zhang, Q. H.; Liu, J. W.; Sager, R.; Dai, L. M.; Baur, J. Hierarchical Composites of Carbon Nanotubes on Carbon Fiber: Influence of Growth Condition on Fiber Tensile Properties. *Compos. Sci. Technol.* **2009**, *69*, 594–601.
- (33) Chen, K. F.; Deng, J. H.; Zhao, F.; Cheng, G. A.; Zheng, R. T. Influence of Zn Ion Implantation on Structures and Field Emission Properties of Multi-Walled Carbon Nanotube Arrays. *Sci. China Technol. Sc.* **2010**, *53*, 776–781.
- (34) Wang, Z. L.; Gao, R. P.; de Heer, W. A.; Poncharal, P. In Situ Imaging of Field Emission from Individual Carbon Nanotubes and Their Structural Damage. *Appl. Phys. Lett.* **2002**, *80*, 856–858.